Scientific Reports

https://doi.org/10.1038/s41598-026-36553-8

Article in Press

Predicting compressive strength of mortars containing recycled CRT glass using GMDH and GEP methods

Received: 8 October 2025

Accepted: 13 January 2026

Published online: 30 January 2026

Cite this article as: Ghorbani V., Seyedkazemi A. & Kutanaei S.S. Predicting compressive strength of mortars containing recycled CRT glass using GMDH and GEP methods. *Sci Rep* (2026). https://doi.org/10.1038/s41598-026-36553-8

Vahid Ghorbani, Ali Seyedkazemi & Saman Soleimani Kutanaei

Predicting Compressive Strength of Mortars Containing Recycled CRT Glass Using GMDH and GEP Methods

Vahid Ghorbani[1], Ali Seyedkazemi[1*], Saman Soleimani Kutanaei[1]

1. *Department of Civil Engineering, Am.C., Islamic Azad University, Amol, Iran*

Abstract

The growing volume of industrial and electronic waste has intensified the need for sustainable material management strategies. Among these waste streams, cathode-ray-tube (CRT) glass is of particular concern due to its high density and lead-bearing composition, which typically contains about 20–25 wt.% lead oxide. Using recycled CRT glass (RCRT) as a fine aggregate in cementitious mixtures offers a practical means of reducing landfill disposal while enhancing mortar performance. However, the mechanical behavior of RCRT-containing mortars has not been sufficiently modeled, thereby constraining the optimized design of such sustainable mixtures. In this study, two white-box, soft-computing techniques, the Group Method of Data Handling (GMDH) and Gene Expression Programming (GEP), were developed to predict the compressive strength of mortars incorporating RCRT. The database consisted of 139 laboratory specimens, and the machine-learning models were trained using the following input variables: water-to-binder ratio (w/b), water content, cement content (CC), fly ash, sand content, RCRT content, and curing time (CT). The GMDH model demonstrated superior predictive performance, achieving an R^2 of 0.942 with RMSE and MAE values of 2.97 and 2.59, respectively. In contrast, the GEP model produced higher error levels (RMSE = 6.94 and MAE = 5.28). These findings indicate that transparent, data-driven modeling can capture the nonlinear interactions governing

* Corresponding Author: E-mail address: ali.seyedkazemi@iau.ac.ir

strength development in RCRT-modified mortars and provides a reliable basis for designing sustainable, dense, and mechanically efficient mixtures suitable for both conventional and radiation-shielding applications.

Keywords: Recycled cathode ray tube; Cement mortar; Compressive strength; Soft computing; Group Method of Data Handling; Gene Expression Programming.

1. Introduction

The development of the electronics industry has led to the production of a large volume of cathode ray tube glass (CRT) waste. The high concentration of heavy metals such as lead in CRT has made its proper disposal a significant environmental challenge. The primary environmental concern associated with CRT waste is lead leaching, as the high lead content poses the most serious risk of contaminating soil and groundwater. Extensive studies conducted using the Toxicity Characteristic Leaching Procedure (TCLP) have shown that CRT waste can result in a significant accumulation of hazardous substances. Therefore, the improper disposal of CRT materials can cause serious environmental issues [1].

Researchers have explored approaches to minimize these risks, and several studies have confirmed that incorporating recycled CRT (RCRT) into alkaline cementitious environments can substantially reduce the leaching of hazardous ions due to the chemical stabilization offered by hydration products [2–3]. The alkaline conditions provided by cement hydration promote chemical binding of heavy metals, and previous research has demonstrated that CRT glass becomes more environmentally stable when incorporated into mortar systems. Zhao and Poon (2017) showed that nitric-acid-treated funnel glass (TFG) can produce mortars with significantly lower drying shrinkage, reduced ASR expansion, and substantially reduced lead leaching, with

all values remaining within regulatory limits. Similarly, Ling and Poon (2011, 2012) reported that processing and particle-size refinement of CRT glass affect shrinkage, fresh properties, and the extent of heavy-metal leaching, confirming the environmental viability of RCRT in alkaline matrices.

Various laboratory studies have examined the use of RCRT as a fine aggregate in mortars, particularly in X-ray and radiation-shielding applications. Gao et al. evaluated the behavior of Portland cement and geopolymer mortars incorporating RCRT. Their findings **showed** that adding RCRT to Portland cement mortars led to a considerable reduction in compressive strength, reaching about 50% in some mixtures, primarily due to significant shrinkage. In contrast, the minimal shrinkage observed in geopolymer mortars **resulted in** only a negligible strength reduction, while heavy-metal leaching and shielding performance remained acceptable, **thereby highlighting** the potential of geopolymer binders for RCRT utilization. Ling and Poon [6] examined the influence of RCRT particle size on both environmental and mechanical characteristics of cement mortar. They reported that the smooth, non-porous surface of RCRT weakened the bond between glass particles and cement paste, resulting in reductions in compressive strength of 10–30%, depending on particle size. At the same time, they observed that the alkaline cement matrix significantly reduced heavy-metal leaching, confirming the environmental viability of RCRT. In another study, Ling and Poon [7] evaluated mortars with 25%, 50%, 75%, and 100% sand-to-RCRT replacement. Their results showed that increasing RCRT content improved workability, reflected in the **increased** of flow spread from about 120 mm to nearly 190 mm, and simultaneously decreased flexural and compressive strengths due to weak particle–paste bonding.

Previous studies have indicated that the high density of recycled CRT glass may enhance X-ray attenuation in cementitious mortars, suggesting potential radiation-related applications (Abouelnour et al., 2025; Mahmoud et al., 2025; Fattouh et al., 2025). Choi et al. [5] and Ling et al. [8] examined the use of recycled CRT glass as a fine aggregate in cementitious mortars and reported that increasing RCRT content can enhance radiation-shielding performance. However, these studies also indicated that such improvements are often accompanied by reductions in mechanical properties, primarily due to weak bonding at the paste–glass interface. These studies provide useful background on the multifunctional potential of RCRT-containing mortars; however, the present work is restricted to mechanical performance, with particular emphasis on compressive strength prediction.

Although previous studies have provided valuable insights into the mechanical, environmental, and shielding performance of RCRT-modified mortars, they also highlight important limitations. Most of the available research **has mainly focused** on experimental results or on studying individual mixture variables, while predictive modeling has received far less attention. At the same time, one of the major challenges in civil engineering, particularly for concretes and mortars incorporating recycled materials, is the reliable prediction of mechanical properties [9-13]. Performing laboratory tests is a costly method to achieve a suitable mixing design. For this reason, researchers have increasingly turned to soft-computing and data-driven methods to estimate the mechanical behavior of cementitious materials containing recycled aggregates (de-Prado-Gil et al., 2024; Ghazavi et al., 2024; Jagadesh et al., 2023; Ghazavi et al., 2025; de-Prado-Gil et al., 2022). These developments highlight the need for accurate and generalizable predictive tools, especially when multiple mixture parameters simultaneously interact and influence mechanical performance simultaneously [14-18].

Ahmad et al. [18] **applied** linear regression models (LRM), nonlinear regression models (NLR), and multilinear regression models (MLR) to predict the compressive strength of mortar containing RCRT. The regression coefficient values of the LRM, NLR, and MLR methods **were reported as** 0.84, 0.87, and 0.85, respectively. Feridoni et al. [19] **employed** GMDH, GEP, and RSM methods to predict the compressive strength of concrete containing recycled brick aggregates. The R^2 values obtained for the GMDH, GEP, and RSM models were 0.84, 0.77, and 0.88, respectively, indicating the promising accuracy of these soft computing techniques. Hoseini et al. [20] used soft computing methods to determine the self-healing properties of self-compacting concrete. The results showed that the initial crack width **was** the most important parameter affecting the self-healing properties. In addition to these studies, de-Prado-Gil et al. (2022) **applied** several ANN-based models to predict the compressive strength of self-compacting recycled aggregate concrete. Their results showed that the ANN models performed well, with the Bayesian Regularization and Levenberg–Marquardt algorithms providing the highest prediction accuracy. They also reported that cement content and water content were the most influential parameters affecting compressive strength.

Although numerous studies have examined cement mortars containing recycled CRT glass and have reported their mechanical, environmental, and radiation-shielding performance, these investigations remain almost entirely experimental and do not provide predictive models for estimating compressive strength. In contrast, existing data-driven approaches in the literature focus only on mortars or concretes incorporating conventional waste glass or recycled aggregates and **primarily** rely on black-box techniques such as ANN or tree-based algorithms. These models are not related to CRT materials and therefore cannot be used to predict the compressive strength of mortars containing recycled CRT glass. Moreover, no research has applied

interpretable (white-box) soft-computing methods, such as GMDH or GEP, to model the mechanical behavior of RCRT-containing mortars. This gap highlights the need for predictive tools that not only achieve high accuracy but also provide explicit mathematical relationships and enable parameter sensitivity assessment. Therefore, the present study aims to (i) develop GMDH and GEP models for predicting the compressive strength of RCRT-modified mortars, (ii) compare their performance with respect to accuracy and interpretability, and (iii) conduct sensitivity analysis to identify the most influential mixture parameters.

2. Database

The selection of input parameters in this study was based on the physical and chemical mechanisms that affect the performance of cement mortars, as well as on previous research on compressive strength (Ling & Poon, 2011; Ling et al., 2012; Zhao & Poon, 2017; Choi et al., 2016). The water-to-binder ratio, water and cement contents, fly ash ratio, natural sand ratio, recycled cathode ray tube glass ratio, and curing time are the main variables that **govern** the hydration reactions, microstructure formation, porosity, and the evolution of compressive strength. Therefore, the selection of these parameters as model inputs is fully consistent with the mechanisms and prior research findings.

The water-to-binder ratio (w/b) is a fundamental factor in cementitious systems and directly affects hydration, microstructure formation, and, ultimately, compressive strength development. The amount of water and cement also influences the workability of the mixture, and the volume of active paste, respectively, which govern the uniform distribution of constituents and, consequently, the mechanical performance. Fly ash, as a pozzolanic material, reacts with hydration products, increasing microstructural density, reducing porosity, and enhancing durability and compressive strength. In this study, recycled cathode ray tube glass (RCRT) was

also used as an alternative fine aggregate; it has been widely reported in previous research to influence both the mechanical and environmental performance of mortars. In addition, curing time is a key parameter that affects the progression of hydration and strength gain, and its significance has been extensively **emphasized** in the literature.

The statistical summary of the input and output data (Table 1) and the histograms (Figure 1) provide important descriptive information, including the mean, standard deviation (StD), coefficient of variation (CoV), and range of variation for each parameter. The variables have different levels of dispersion, which can be seen through their StD and CoV. As the target variable, the compressive strength also **exhibits** a sufficiently wide variability with a CoV of 37.62%, which is suitable for developing predictive models. Notably, some parameters such as Sand, RCRT, and curing time exhibit relatively high coefficients of variation (CoV), indicating that the dataset covers a wide range of mixture proportions and curing durations. Such variability is typical in studies involving recycled materials and non-standardized mix designs and reflects the **heterogeneous nature of the collected mixtures**. To ensure the reliability and consistency of the data, the Modified Z-score method with a threshold of 3.5 was applied to identify and remove potential outliers. This procedure was performed on the input variables w/b, water, CC, fly ash, Sand, RCRT, and CT to detect any anomalous values within the dataset.

After removing the outliers, all input variables were normalized using Z-score normalization (Zhang et al., 2024; Aksu et al., 2019; Safieh et al., 2024; Raju et al., 2024) to place the features on a comparable scale and to prevent parameters with high numerical dispersion from dominating the model training process.

Table 1.
Statistical information related to input and output data.

Variable	Total Count	Mean	StD	Variance	CoV	Min	Max
w/b	139	0.42842	0.04129	0.00170	9.64	0.35	0.45
Water (kg/m³)	139	268.32	9.13	83.42	3.40	250	273.6
Cement content (kg/m³)	139	497.01	85.89	7376.88	17.28	456	721
Fly ash (kg/m³)	139	134.63	47.08	2216.06	34.97	0	152
Sand (kg/m³)	139	597.3	553.3	306126.4	92.63	0	1520
RCRT (kg/m³)	139	938.0	631.5	398752.1	67.32	0	1734
Curing time (days)	139	30.29	33.26	1106.47	109.80	1	91
Compressive strength (MPa)	139	33.91	12.76	162.75	37.62	7.73	59.36

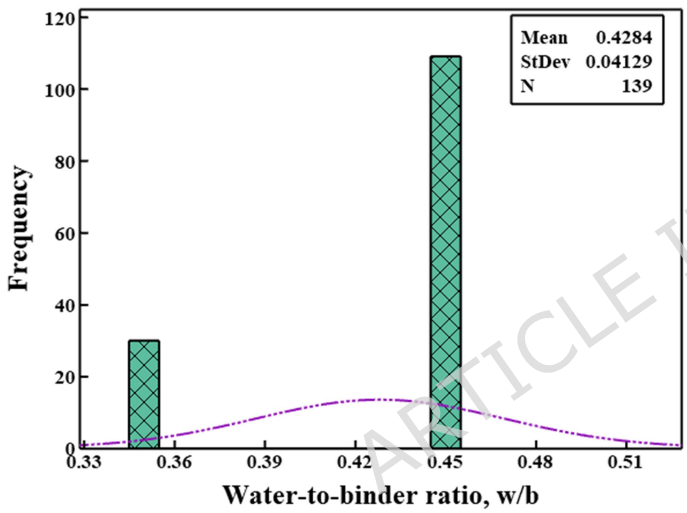

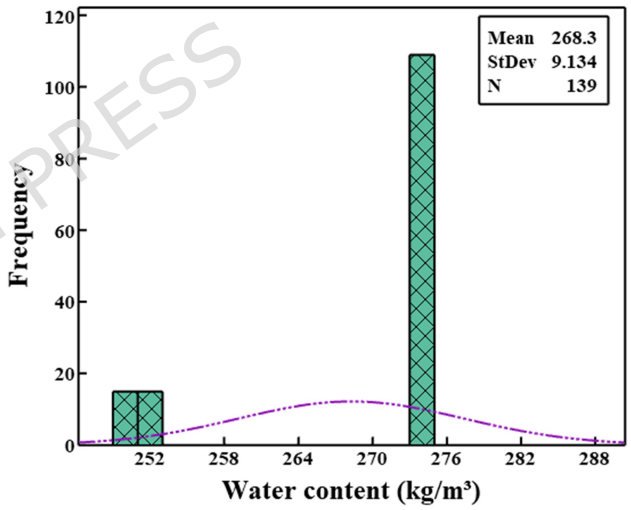

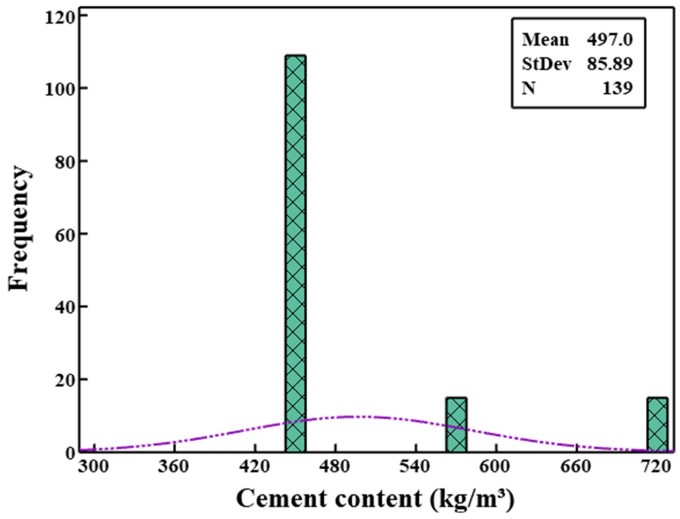

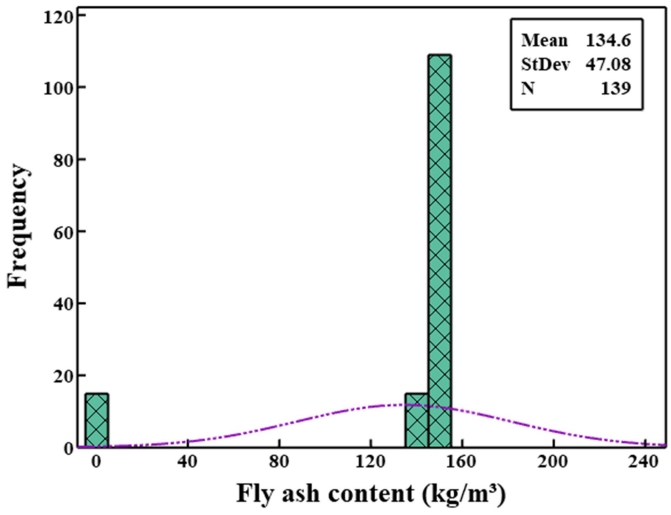

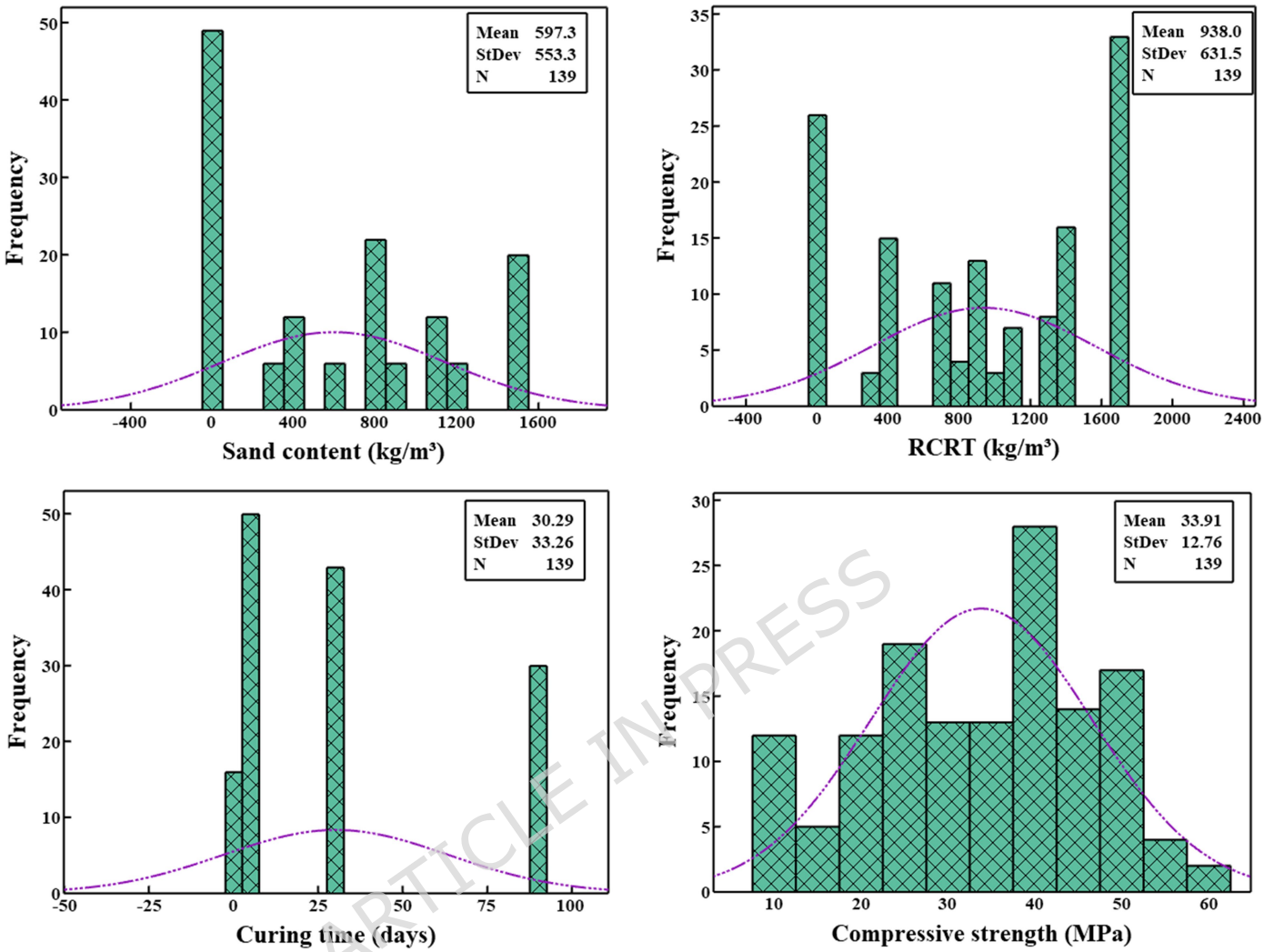

Figure 1. Histograms of each input and output variable along with their corresponding distribution curves.

3. Soft computing modeling

3.1. Group Method of Data Handling method

The GMDH method is a white-box, equation-based soft computing algorithm that models complex systems and identifies nonlinear relationships between variables (Ivakhnenko, 2007; Farlow, 2020). GMDH is a multilayer, network-based modeling approach that predates modern neural networks and is considered one of the earliest self-organizing learning algorithms. A key

advantage of GMDH is its ability to generate explicit and interpretable polynomial equations that describe the relationships between input and output variables (Ivakhnenko & Ivakhnenko, 1995). The GMDH process involves iteratively generating layers of candidate models, typically in the form of second-order polynomial neurons constructed from pairs of input variables. In each layer, the polynomial coefficients are estimated using the training subset, while model selection is performed using the **validation subset error**. Specifically, all candidate neurons are ranked according to their root-mean-square error on the validation data, and only the best-performing neurons are retained for the next layer. This validation-based criterion helps maintain a balance between model accuracy and structural complexity by automatically pruning weak nodes (Farlow, 2020; Babin et al., 2025). The iterative process continues until only a single neuron remains in the final layer, which represents the optimal model with the lowest validation error. Thanks to this self-organizing structure and the use of a separate validation subset, the GMDH algorithm effectively reduces overfitting and **produces** models with strong generalization capability.

Similar observations about the effectiveness and generalization ability of intelligent soft-computing models have also been reported in recent studies that employed Artificial Neural Networks (ANN), Genetic Algorithms (GA), the Water Cycle Algorithm (WCA), and Fuzzy Logic for concrete prediction tasks (Mahmoud et al., 2025; Dahish et al., 2025; Fathy et al., 2025; Mahmoud et al., 2025; Zeyad et al., 2024).

A total of 139 laboratory samples was used to develop the predictive models. In accordance with common practice in soft-computing–based modeling, 80% of the data were randomly selected for training and the remaining 20% were used for testing to evaluate model performance

(Fereidouni et al., 2025; Hosseini et al., 2025; Ghazavi & Afrakoti, 2025; Akossou & Palm, 2013; Fallahi et al., 2015).

In this study, the GMDH model was developed to predict the compressive strength of RCRT-modified mortar. The optimal structure of the model **consisted** of four layers with 20 neurons in each layer. This architecture was selected through a trial-and-error procedure to achieve the highest prediction accuracy. Table 2 presents descriptive statistics, including minimum, maximum, and mean values in both the training and test sets, to better understand the statistical properties of the input and output data. This information provides an initial understanding of the diversity and range of variables used.

Table 2.
Descriptive statistics of variables used in the GMDH method

Variable		Train (111 data)			Test (28 data)		
		Min	Mean	Max	Min	Mean	Max
Inputs	w/b	0.35	0.43	0.45	0.35	0.4214	0.45
	Water (kg/m^3)	250	268.65	273.6	250	266.82	273.6
	Cement content (kg/m^3)	456	492.63	721	456	515.64	721
	Fly ash (kg/m^3)	0	137.2	152	0	123.89	152
	Sand (kg/m^3)	0	608.10	1520	0	576.35	1520
	RCRT (kg/m^3)	0	931.26	1734	0	936.25	1734
	Curing time (days)	1	29.59	91	1	34.107	91
Output	Compressive strength (MPa)	11.752	33.35	54.206	11.752	35.86	50.93

Figure 2 shows the final architecture of the developed GMDH model. As shown, the model consists of four hidden layers, with a maximum of 20 nodes (neurons) generated in each layer. However, only the nodes that **achieved** the best prediction performance (based on the minimum validation error) **were transferred** to the subsequent layers. This automatic selection of nodes is a key feature of the GMDH method that **helps prevent** overfitting.

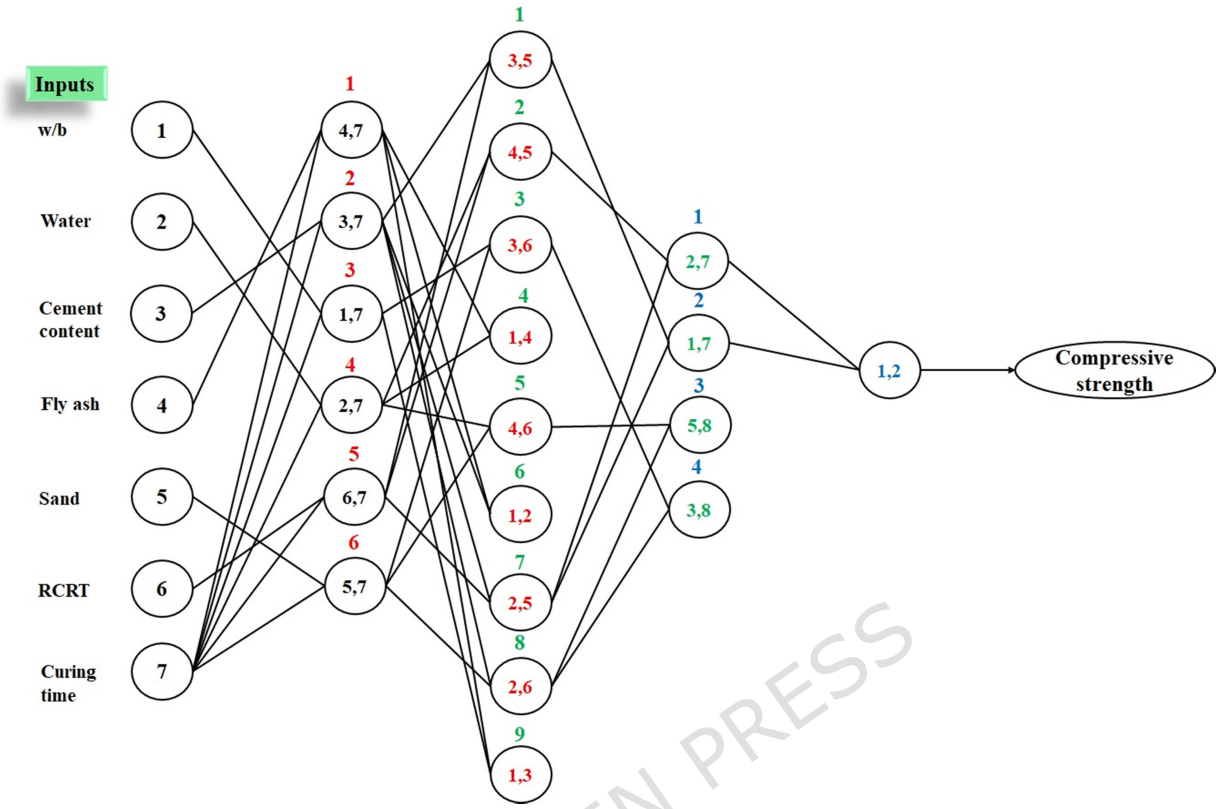

Figure 2. The evolved structure of the GMDH generalized neural network

Based on the optimal model structure presented in Figure 2, the selected nodes in each layer are constructed using a nonlinear combination of two input variables **in the form of** quadratic polynomials. **The equations corresponding to the selected nodes in the different layers are presented** in Eq. 1. These equations show how the compressive strength of RCRT-modified mortar **is computed** stepwise from the initial inputs and the outputs of the intermediate layers.

$$
\begin{aligned}
y_1 &= -73.78 + 0.291 \times CC + 1.139 \times CT - 0.0002 \times CC^2 - 0.0058 \times CT^2 - 0.0006 \times CC \times CT \\
y_2 &= 65.45 - 75.049 \times w/b + 0.233 \times CT - 70.348 \times w/b^2 - 0.0058 \times CT^2 + 1.422 \times w/b \times CT \\
y_3 &= -690.22 + 6.051 \times water - 0.887 \times CT - 0.0126 \times water^2 - 0.0059 \times CT^2 + 0.00646 \times water \times CT \\
y_4 &= 21.641 + 0.00102 \times RCRT + 0.9605 \times CT - 3.1 \times 10^{-6} \times RCRT^2 - 0.00688 \times CT^2 - 1.3 \times 10^{-5} \times RCRT \times CT
\end{aligned} \tag{1a}
$$

$$
\begin{aligned}
Y_1 &= -15.595 + 1.98 \times y_2 - 0.0047 \times y_4 + 0.0054 \times y_2^2 + 0.0349 \times y_4^2 - 0.0544 \times y_2 \times y_4 \\
Y_2 &= -15.609 + 1.943 \times y_3 + 0.0321 \times y_4 + 0.00571 \times y_3^2 + 0.0342 \times y_4^2 - 0.0537 y_3 \times y_4 \\
Y_3 &= -17.599 + 2.131 \times y_1 - 0.0171 \times y_4 - 0.0047 \times y_1^2 + 0.0261 \times y_4^2 - 0.0374 \times y_1 \times y_4
\end{aligned} \tag{1b}
$$

$$
\begin{aligned}
\bar{Y}_1 &= -4.299 - 9.415 \times Y_2 + 10.692 \times Y_3 + 0.981 \times Y_2^2 + 0.704 \times Y_3^2 - 1.69 \times Y_2 \times Y_3 \\
\bar{Y}_2 &= -6.303 - 10.521 \times Y_1 + 11.938 \times Y_3 + 0.778 \times Y_1^2 + 0.458 \times Y_3^2 - 1.243 \times Y_1 \times Y_3
\end{aligned} \tag{1c}
$$

$$
\text{Compressive strength} = -1.873 - 8.29 \times \bar{Y}_1 + 9.32 \times \bar{Y}_2 + 3.818 \times \bar{Y}_1^2 + 3.65 \times \bar{Y}_2^2 - 7.469 \times \bar{Y}_1 \times \bar{Y}_2 \tag{1d}
$$

3.2. Gene Expression Programming method

The GEP method is an evolutionary algorithm from the family of soft computing, derived from the principles of genetic evolution, designed to model complex and nonlinear relationships between variables (Ferreira, 2001; Ghanizadeh et al., 2024; Ghazavi & Afrakoti, 2025). This method combines the advantages of Genetic Algorithms (GA) and Genetic Programming (GP). It uses a fixed-length chromosome representation of mathematical functions and operators and can automatically generate explicit mathematical equations for output prediction (Ferreira, 2006; Ferreira, 2009). In GEP, each chromosome contains genes that are translated into expression trees (ETs), and then through natural selection, mutation, and recombination, optimized models with minimal errors are produced (Faraz et al., 2023). These features make GEP a white-box, equation-based method not only in terms of accuracy but also in terms of the interpretability of its model structure. Its high flexibility, ability to identify hidden relationships, and capability to

extract explicit mathematical functions have made GEP an efficient tool for engineering applications (Alabduljabbar et al., 2023; Ghanizadeh et al., 2024). To better understand the statistical characteristics of the input and output data used in the GEP method, Table 3 presents descriptive statistics, including minimum, maximum, and mean values in both the training and testing datasets.

Table 3.
Descriptive statistics of variables used in the GEP method

Variable		Train (111 data)			Test (28 data)		
		Min	Mean	Max	Min	Mean	Max
Inputs	w/b	0.35	0.4247	0.45	0.35	0.442	0.45
	Water (kg/m^3)	250	267.509	273.6	250	271.53	273.6
	Cement content (kg/m^3)	456	503.927	721	456	469.57	721
	Fly ash (kg/m^3)	0	131.693	152	0	146.25	152
	Sand (kg/m^3)	0	550.729	1520	0	782.107	1520
	RCRT (kg/m^3)	0	978.171	1734	0	778.96	1734
	Curing time (days)	1	29.324	91	1	34.142	91
Output	Compressive strength (MPa)	7.73	34	59.36	9.12	33.576	52.16

In order to investigate the performance of the GEP method in predicting compressive strength, three different models were developed with different parameter settings, the specifications of which are presented in Table 4. These models used different mathematical base functions (including trigonometric, exponential, logarithmic, and inverse functions), and **also differed** in head size, number of genes, mutation rate, and gene combination rates. Moreover, three different fitness functions including Relative Absolute Error (RAE), Root Mean Square Error (RMSE), and Root Relative Squared Error (RRSE) were tested because each measures prediction error in a distinct way, allowing the algorithm to determine which criterion provides the most stable and accurate learning behavior for the variability present in the dataset. A comparison of the R^2

values in the training and testing phases clearly shows that Model-1 achieved the highest prediction accuracy among the three configurations. This model established a strong agreement between the actual and predicted values , with R^2=0.734 for the training data and R^2=0.758 for the testing data. These results indicate that Model-1 **has greater accuracy** and **more stable** prediction performance than the other two models and can be considered the selected model for further analyses.

Table 4.
Parameters used in the GEP model

Parameter	Definition	Model-1	Model-2	Model-3
P1	Fitness Function	RAE	RMSE	RRSE
P2	Function set	+, -, ×, /, Sin, Cos, Atan	+, -, ×, /, Exp, X^2, Inv	+, -, ×, /, Inv, X^2, X^3
P3	Chromosomes	30	20	40
P4	Head size	8	6	5
P5	Number of genes	4	4	6
P6	Linking function	Addition	Addition	Addition
P7	Mutation rate	0.0588	0.0856	0.0136
P8	Inversion rate	0.1	0.1	0.1
P9	One-point recombination rate	0.2	0.1	0.2
P10	Two-point recombination rate	0.2	0.1	0.3
P11	Gene recombination rate	0.3	0.5	0.2
P12	Gene transposition rate	0.1	0.1	0.1
P13	Constant per gene	10	10	10
P14	Training-R^2	0.734	0.675	0.653
P15	Testing-R^2	0.758	0.698	0.729

The final equation of the selected GEP model (Model-1) is as Eq. 2.

$$\text{Compressive strength} = \left[\frac{7.0152}{\text{Arc}\tan\left(\text{w}/\text{b}\right)}\right] + \left[\frac{3.66}{\text{Arc}\tan\left(\text{w}/\text{b}\right)}\right] + \ldots \left[\text{Arctan}\left(\left(1.121-7.473\right)\times\left(\text{w}/\text{b}\times\text{CT}\right)\right) + \cos\left(\frac{\text{RCRT}-1.121}{\text{CC}}\right)\right] + \ldots \left[\cos\left(\cos\left(\left(\text{fly ash}\times\text{w}/\text{b}\right)\times\left(-9.729\right)\right)\right)\times\left(\text{w}/\text{b}\times\text{CT}\right)\right] \quad (2)$$

To better understand the mathematical structure of the model, Eq. 2 **is also presented** in the ETs form in Figure 3, where the root represents the primary operator and the branches terminate in the input functions and variables. This representation **helps to better illustrate** the nonlinear and nested relationships between the parameters and the output.

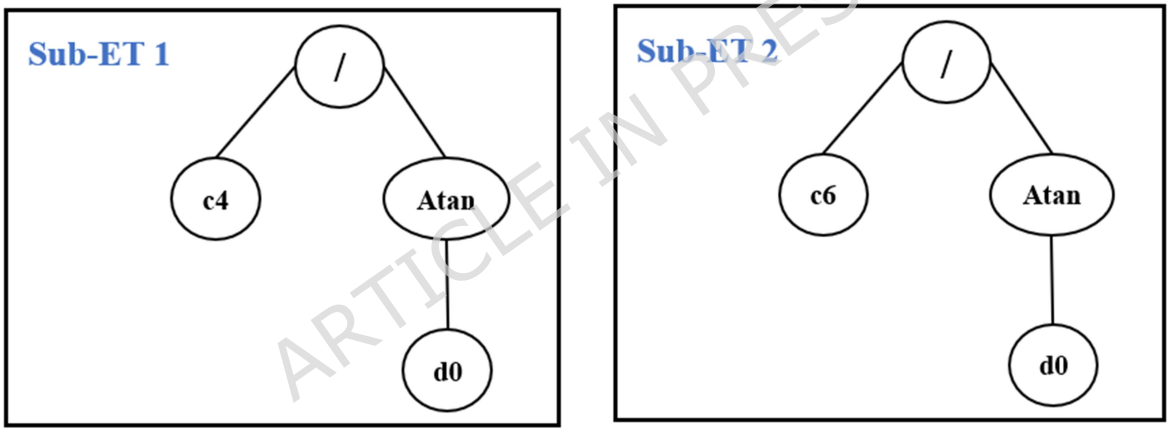

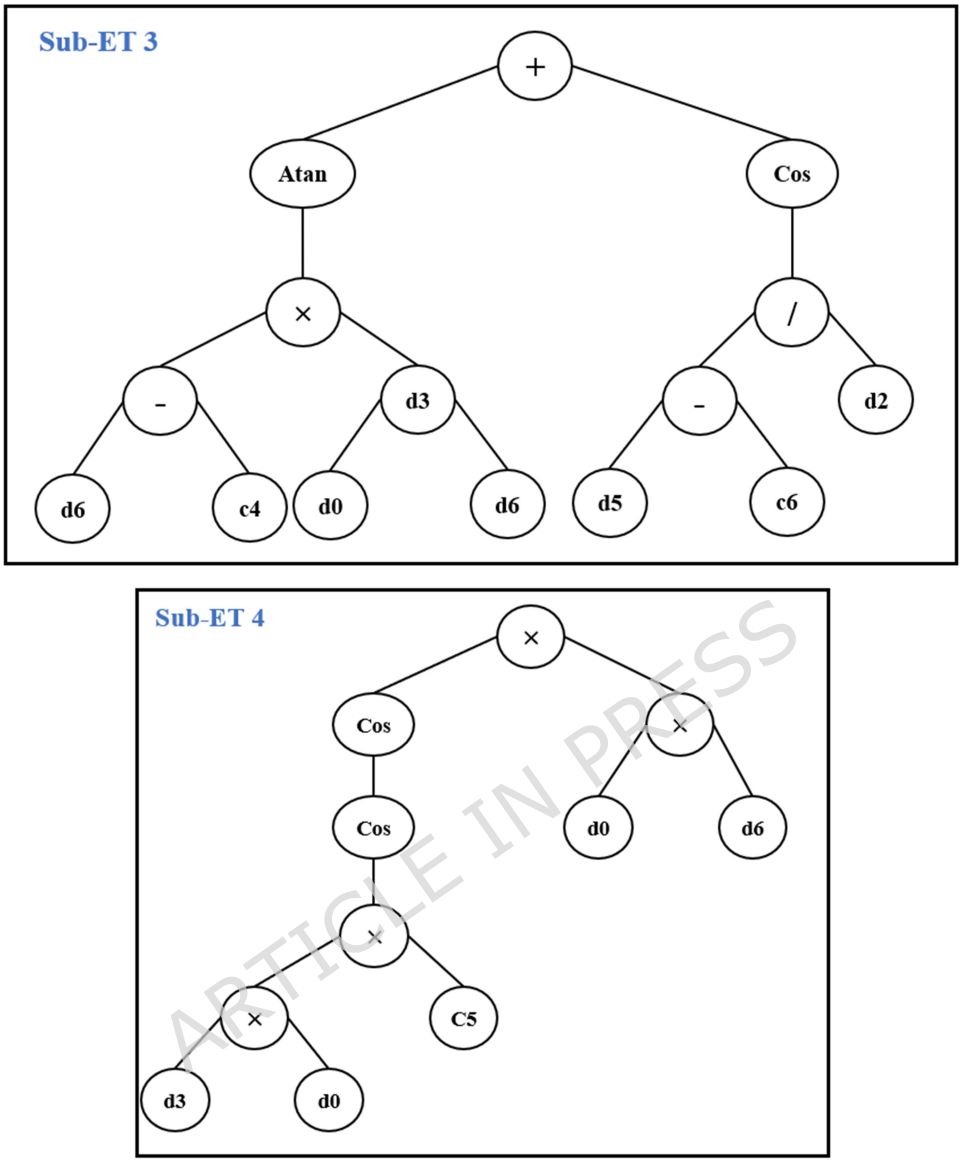

Figure 3. ETs representation of the Eq.2 for predicting the compressive strength of RCRT-modified mortar.

3.3. Interpretability and Practical Applicability of the Proposed Equations

Previous studies employing white-box and transparent (equation-based) models to predict the behavior of complex engineering materials, particularly concrete, have commonly led to the formulation of relatively extensive mathematical relationships. This outcome mainly reflects the

use of nested polynomial structures required to capture the inherent complexity of such materials. In several studies, methods such as GMDH and GEP have been explicitly referred to as white-box approaches due to their ability to provide explicit and extractable mathematical expressions (Amar & Ghahfarokhi, 2020; MolaAbasi et al., 2021). Accordingly, the complexity of the derived equations should be interpreted as a reflection of the inherent complexity of concrete behavior rather than as a limitation of the modeling approach.

The resulting equations, despite involving multiple terms, remain practically usable due to their explicit structure, which allows straightforward implementation in common computational tools such as Microsoft Excel. In practical engineering applications, such formulations enable rapid evaluation of multiple mix design scenarios with minimal computational effort. Consequently, equation-based models provide an efficient analytical framework for strength prediction and optimization tasks, particularly when repeated calculations are required, offering a practical alternative to purely black-box approaches (Ashrafian et al., 2020; Pham, 2025).

4. Model Performance Evaluation

4.1. Performance Assessment and Comparative Modeling Analysis

To investigate the accuracy, efficiency, and generalizability of the developed models in compressive strength prediction, the performance of two white-box computational methods, including GMDH and GEP, was evaluated in comparison with classical regression models, including linear regression (LR), nonlinear regression (NLR), and multiple linear regression (MLR). This evaluation was carried out using statistical indices **such as** R^2, MAE, RMSE, and the scatter index (SI). Comparing these indices in the training and testing datasets **provides** a clearer understanding of model accuracy, error dispersion, and generalizability.

$$R^2 = 1 - \left[\frac{\sum_{i=1}^{N} (y_i - \hat{y}_i)^2}{\sum_{i=1}^{N} (y_i - \bar{y})^2} \right] \quad (3a)$$

$$RMSE = \sqrt{\frac{\sum_{i=1}^{N} (y_i - \hat{y}_i)^2}{N}} \quad (3b)$$

$$\mathrm{SI} = \frac{\mathrm{RMS}}{\bar{\mathrm{y}}} \quad (3c)$$

$$MAE = \frac{\sum_{i=1}^{N} |y_i - \hat{y}_i|}{N} \quad (3d)$$

Figures 4 to 7 graphically compare the prediction accuracy of the different models based on statistical indices such as R^2, MAE, RMSE, and SI. The results **indicated** that the GMDH model performed best among all methods. In the test data, its R^2 value was 0.942, which was higher than that of all other models, and it achieved the lowest RMSE and MAE values of 2.97 and 2.59, respectively. The GEP model also showed acceptable performance but with lower accuracy and generalizability than GMDH. In contrast, the classical regression models, including LR, NLR, and MLR, **performed** poorly, especially the simple linear model (LR), whose R^2 value **was reported to be** lower than 0.72. This difference in performance **demonstrates** that classical methods have limitations in modeling the nonlinear and complex relationships between input parameters and compressive strength (Ahmad et al., 2021; Kontoni et al., 2022; Aslam et al., 2020). In addition, the SI index showed that the GMDH model had the lowest SI in the test data (0.993), indicating a high level of agreement between the model predictions and the actual values. Although the GEP model, with **SI = 0.843**, performed relatively well, it **still exhibited** lower accuracy than GMDH.

In contrast, the classical regression models, particularly the LR model with SI = 0.116, **exhibited** considerably weaker predictive accuracy, further highlighting the superiority of white-box methods under complex and nonlinear conditions. The superiority of the GEP and GMDH soft-computing methods **lies in their capability** to identify and model complex nonlinear relationships without requiring a specific functional form or statistical assumptions (Ahmad et al., 2021; Kontoni et al., 2022; Elshaarawy et al., 2024). Unlike black-box techniques such as neural networks, these methods are white-box and generate interpretable mathematical equations or tree structures that **improve** scientific understanding of the underlying behavior. In addition, their high structural flexibility, capability to learn from experimental data, generalization to unseen conditions, and robustness to noise **provide** further advantages over traditional models. Overall, soft-computing methods, particularly for problems involving multivariate and nonlinear relationships such as compressive strength prediction, offer a powerful and effective approach that delivers more accurate, stable, and reliable results than classical regression models.

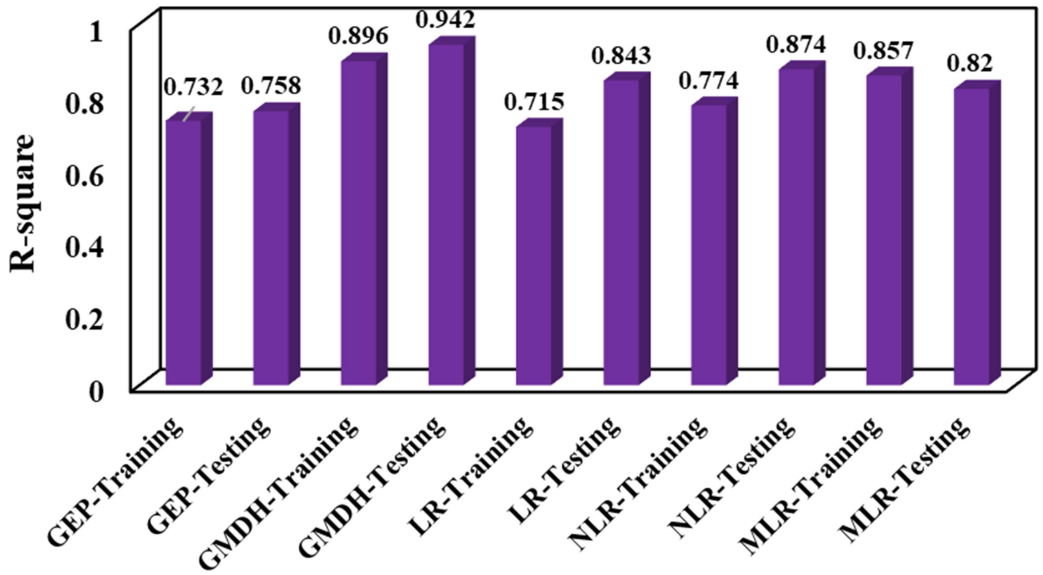

Figure 4. R^2 of different models including GEP, GMDH, LR, NLR and MLR on training and testing data for predicting compressive strength.

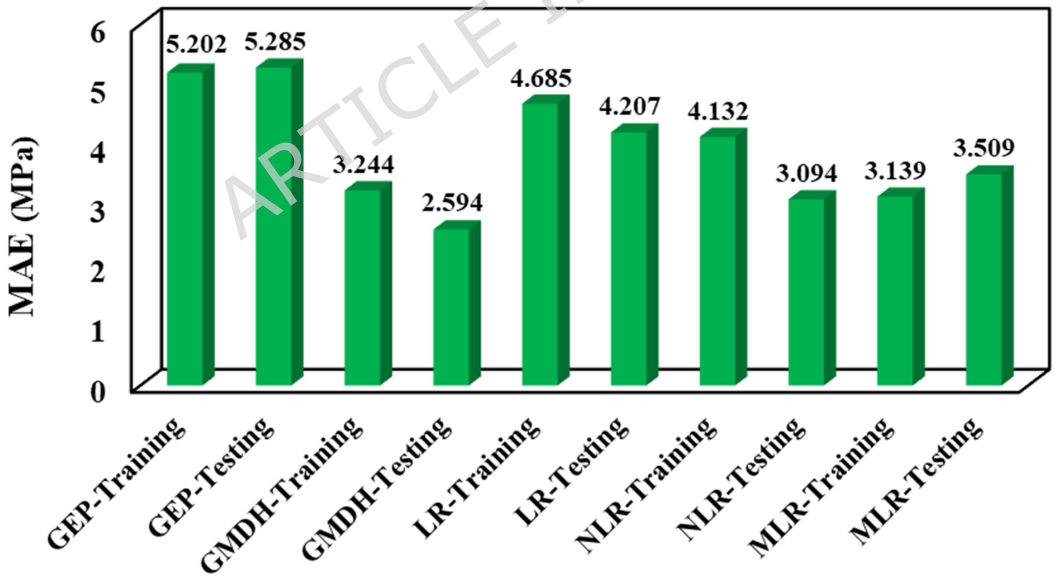

Figure 5. MAE of different models including GEP, GMDH, LR, NLR and MLR on training and testing data for predicting compressive strength.

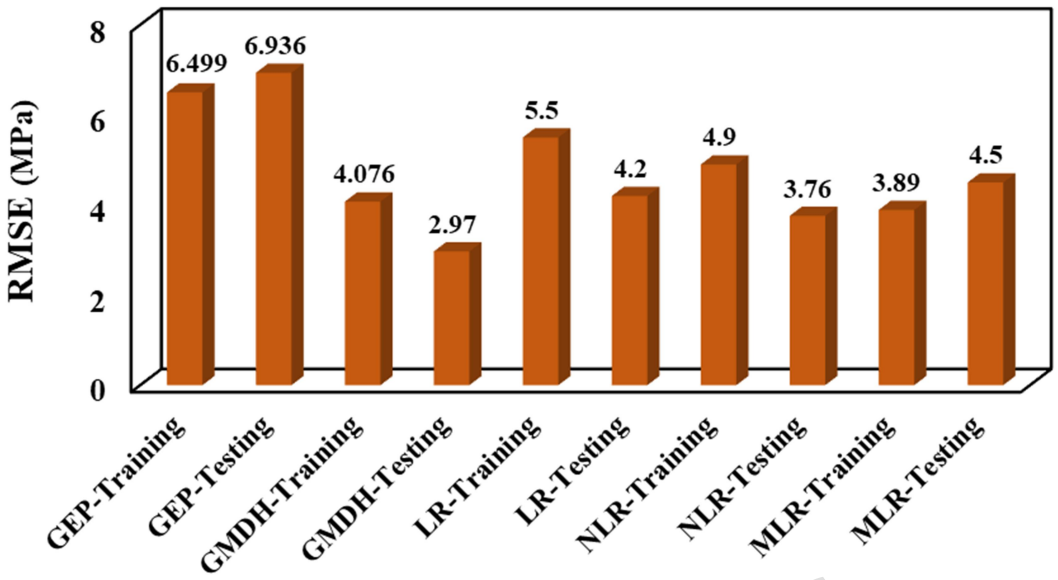

Figure 6. RMSE of different models including GEP, GMDH, LR, NLR and MLR on training and testing data for predicting compressive strength.

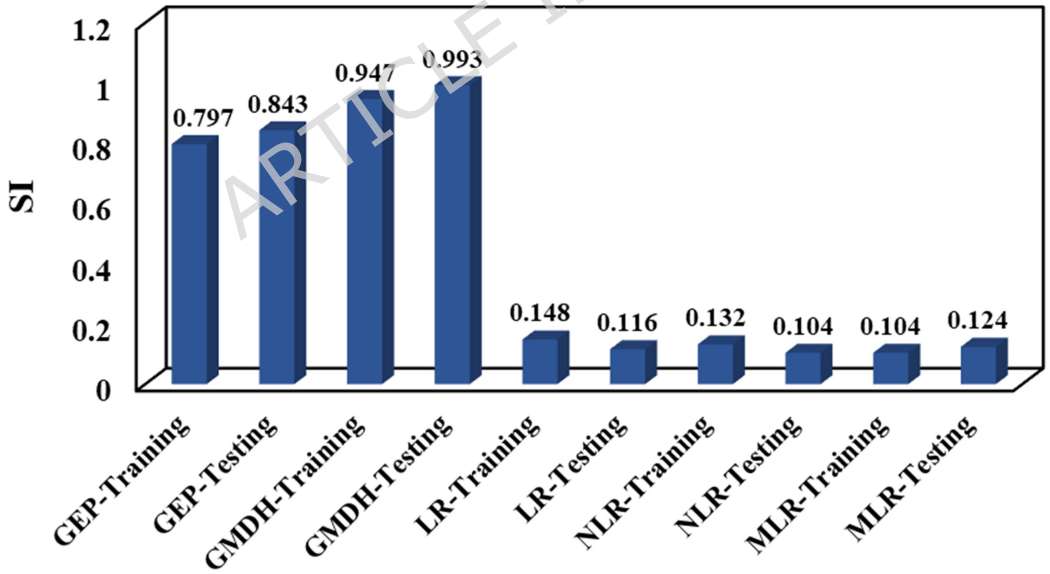

Figure 7. SI of different models including GEP, GMDH, LR, NLR and MLR on training and testing data for predicting compressive strength.

Figures 8 to 10 include a scatter plot of the predicted and actual data, the absolute error, and a regression plot to compare the performance of the two soft-computing models, GEP and GMDH, in predicting compressive strength.

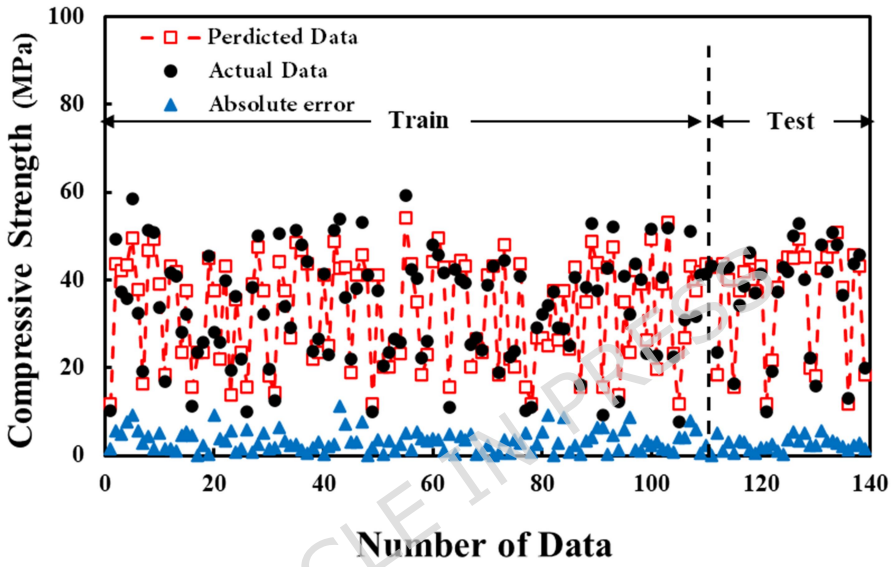

Figure 8. Comparison between actual and predicted compressive strength data with absolute error for the GMDH model.

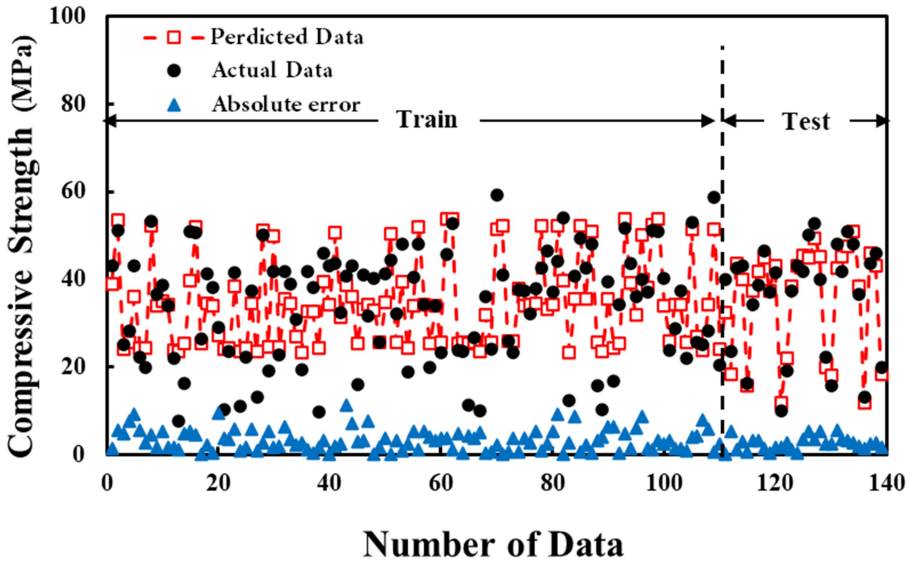

Figure 9. Comparison between actual and predicted compressive strength data with absolute error for the GEP model.

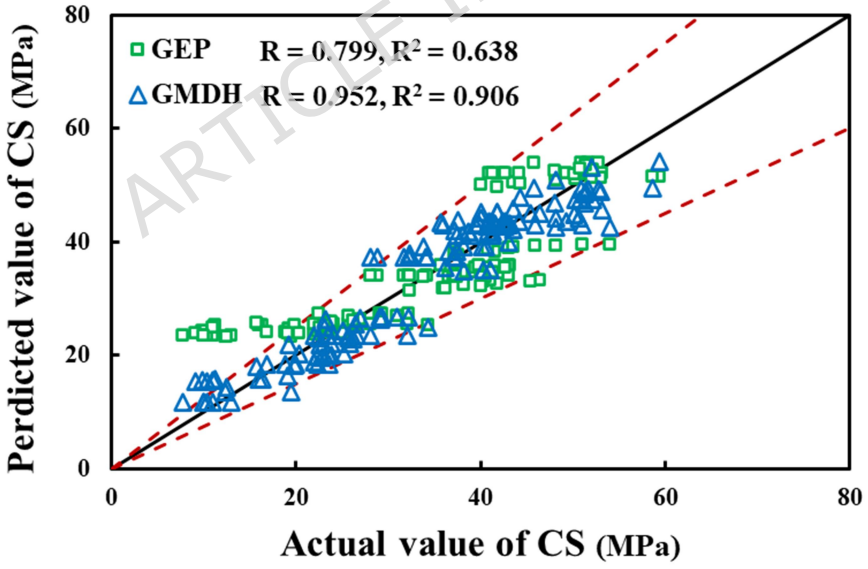

Fig 10. Comparison between actual and predicted compressive strength values using GEP and GMDH models.

Figures 8 and 9 show that the GMDH model **reconstructed** the compressive strength values with higher accuracy. The predicted points closely matched the actual values, and the absolute error **remained** low. In contrast, the GEP model showed greater fluctuations in the output and higher error dispersion, indicating that it **was less accurate than the GMDH model**.

The regression plot (Figure 10) depicts the correlation between the actual and predicted values for both models based on **the entire dataset**. The GMDH model, with $R^2 = 0.906$ and $R = 0.952$, established a strong relationship close to the ideal line between the actual and predicted data. In contrast, the GEP model, with lower values **($R^2 = 0.638$ and $R = 0.799$)**, performed worse in reconstructing the actual trend of compressive strength. These results **are consistent with** the statistical indicators presented in the previous section and confirm the superiority of the GMDH model over GEP in terms of accuracy, stability, and generalizability.

To further evaluate the predictive performance and error behavior of the developed models, a residual analysis was performed. **Figure 11 illustrates** the distribution of residuals (Actual – Predicted) for the GEP and GMDH models, respectively.

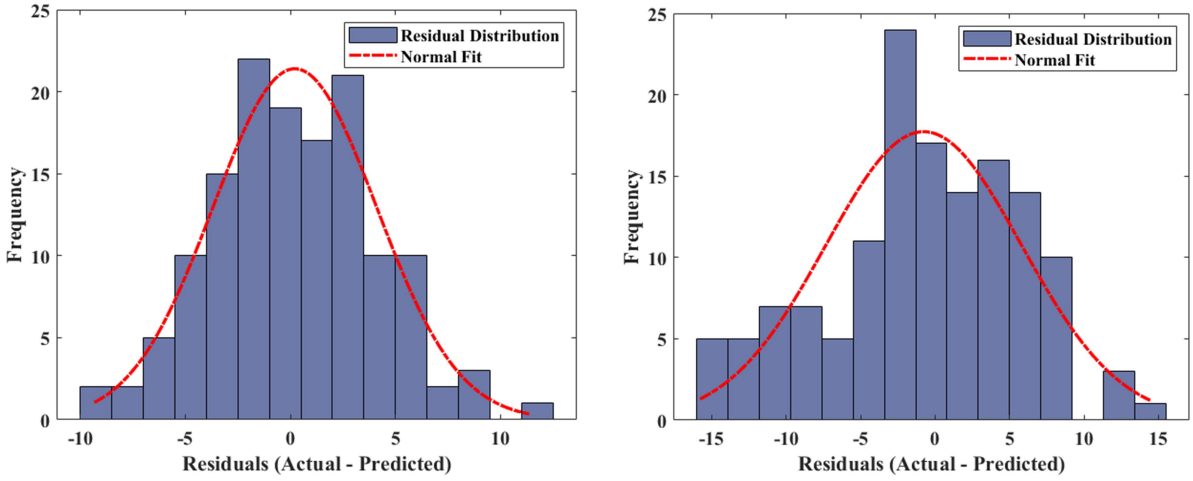

(a) (b)

Figure 11. Residual distributions for the models: (a) GEP model; (b) GMDH model.

The histogram and normal–fit curve for the GEP model show that its residuals are widely scattered and deviate from a normal pattern, indicating higher variability and the presence of larger prediction errors. This confirms that the GEP model is less stable and exhibits weaker generalization capability. In contrast, the residual distribution of the GMDH model is more compact and closely follows a **near-normal** bell-shaped curve centered around zero. This pattern indicates that the prediction errors are smaller, more symmetrically distributed, and free from systematic bias. These findings are consistent with the higher R^2 values and lower error statistics produced by the GMDH model and further **confirm** its superior accuracy and robustness compared with the GEP model.

4.2 Analysis of K-fold Cross-Validation

To more precisely assess the stability and generalizability of the two soft-computing models, GMDH and GEP, a 5-fold cross-validation process was conducted. The results of this analysis are presented in Figure 12 **using** a spider plot.

Figure 12 illustrates that the GMDH model exhibits a relatively homogeneous and stable behavior in all folds. The R^2 values range from 0.82 to 0.93, indicating consistently high predictive capability. Moreover, the RMSE values across folds range from 2.09 to 4.47 MPa. The MAE index also shows the model's accurate and stable performance, with values of 3.45, 3.17, 3.57, 3.29, and 1.72 MPa, respectively. Furthermore, the SI for different folds ranges from 0.17 to 0.31. These patterns **confirm that the GMDH model is robust to** variations in data partitioning and **demonstrates** consistent overall behavior.

In contrast, the GEP model showed less stable performance, with greater variability. The R^2 values of this model ranged from 0.52 to 0.68 across folds, indicating inconsistent predictive performance. Furthermore, the RMSE index **showed** much higher values, ranging from 6.28 to 10.47 MPa. The MAE (from 5.13 to 8.43 MPa) and SI (from 0.47 to 0.75) indices also **confirmed** the higher sensitivity and weaker generalizability of the GEP model compared with the GMDH model.

Overall, the K-fold cross-validation analysis results clearly demonstrated that the GMDH model is more stable, accurate, and reliable across all indices and outperforms the GEP model in predicting compressive strength.

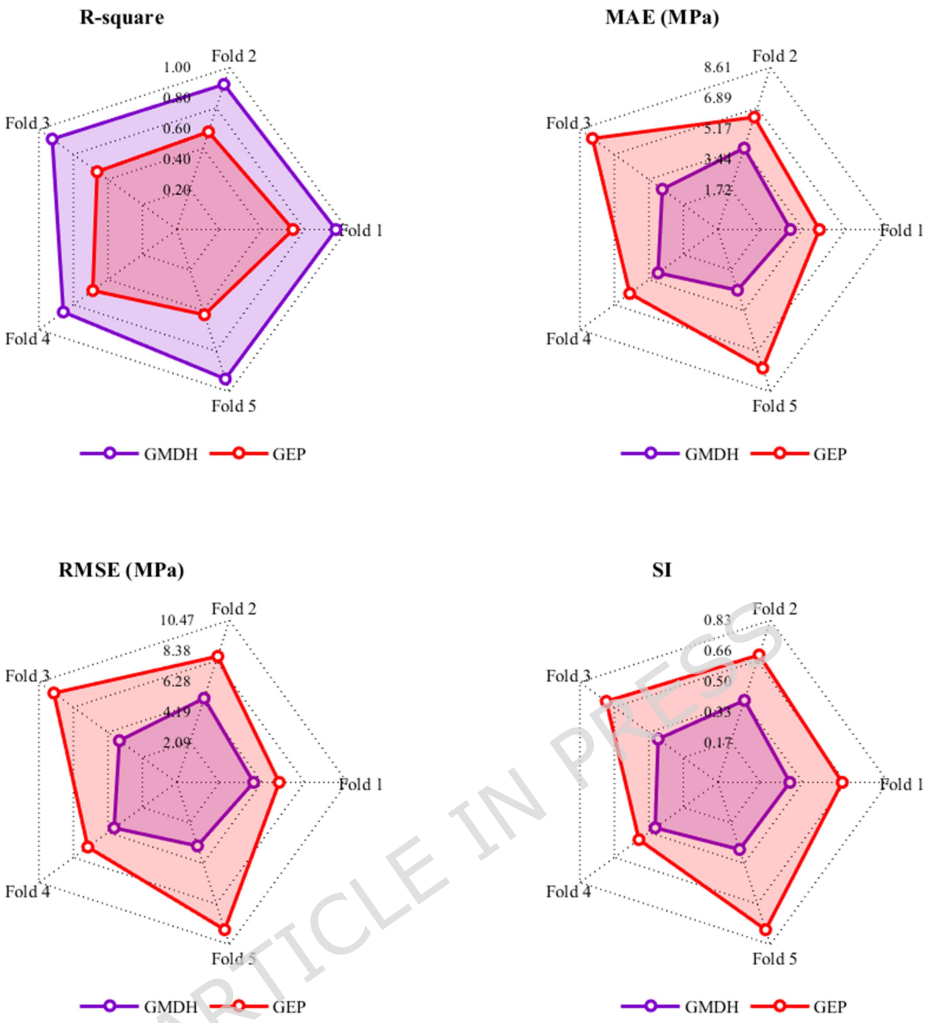

Figure 12. Five-fold cross-validation performance of the GMDH and GEP for four statistical metrics (R^2, RMSE, MAE, and SI).

4.3. Sensitivity analysis

To evaluate the relative influence of the input parameters on the predicted compressive strength, a SHAP-based sensitivity analysis was performed. SHAP (SHapley Additive exPlanations) provides a global, scale-independent interpretation of model behavior and quantifies how much each input contributes to the final prediction. Unlike traditional perturbation approaches, SHAP

inherently normalizes the effects of variables with different units and magnitudes, ensuring an unbiased comparison among parameters.

Figure 13 shows the SHAP feature contribution scores for the GMDH model. According to these results, water content was identified as the most influential variable, contributing more than any other parameter to the variation in compressive strength. This is consistent with the fundamental role of water in controlling the water-to-binder environment, hydration kinetics, pore structure development, and the formation of the C–S–H gel (Ling & Poon, 2011; Choi et al., 2016). This finding **is consistent with** previous ML-based studies, where the water-to-binder (or water-to-cement) ratio has been consistently reported as the dominant factor governing strength development (Wan et al., 2021; Meng et al., 2025; Shuai et al., 2025).

Curing time (CT) was ranked as the second most influential parameter, highlighting its critical role in strength gain through the progressive hydration process (Shanthi Vengadeshwari et al., 2025; Ashraf et al., 2024). Cement content (CC) showed a moderate contribution, consistent with prior data-driven and experimental studies that emphasize the secondary role of binder dosage in recycled-aggregate systems (Ahmad et al., 2021; de Prado-Gil et al., 2022)**.**

In contrast, RCRT content and the w/b ratio showed smaller effects on strength, which is consistent with earlier studies reporting that CRT glass mainly affects mechanical behavior through its particle shape and weak interfacial bonding rather than chemical reactivity (Zhao & Poon, 2017; Ling & Poon, 2013).

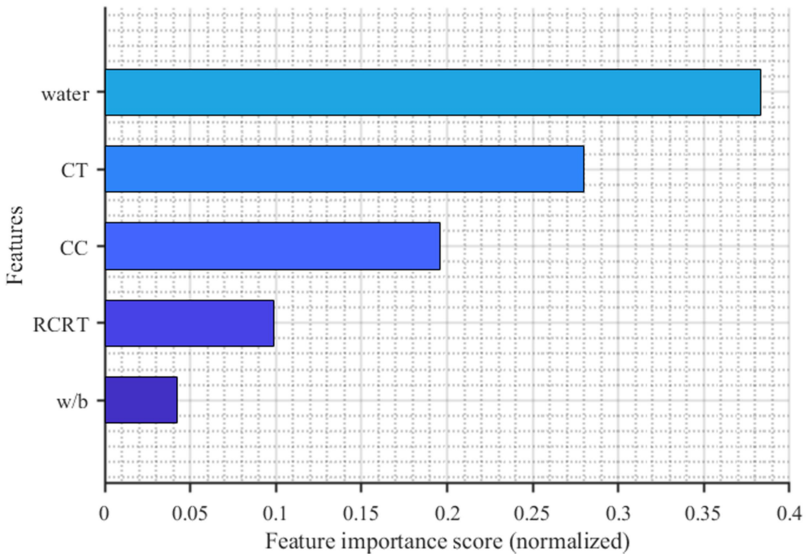

Figure 13. Global SHAP-based feature contribution scores for input variables affecting compressive strength.

To gain further insight into the directional impact of each variable, SHAP dependence plots were generated (Figure 14). These plots illustrate how changes in individual input parameters affect their corresponding SHAP values. For example, an increase in water content generally produced negative SHAP values, indicating a reduction in compressive strength due to increased porosity and dilution effects (Ling & Poon, 2011; Wan et al., 2021; Meng et al., 2025). Conversely, longer curing times resulted in positive SHAP values, reflecting the expected improvement in strength with extended hydration (Choi et al., 2016; Shanthi Vengadeshwari et al., 2025). The dependence plots for CC and RCRT showed more localized and nonlinear behaviors, highlighting their secondary but meaningful contributions to strength development (Zhao & Poon, 2017; Ling & Poon, 2013; Ashraf et al., 2024).

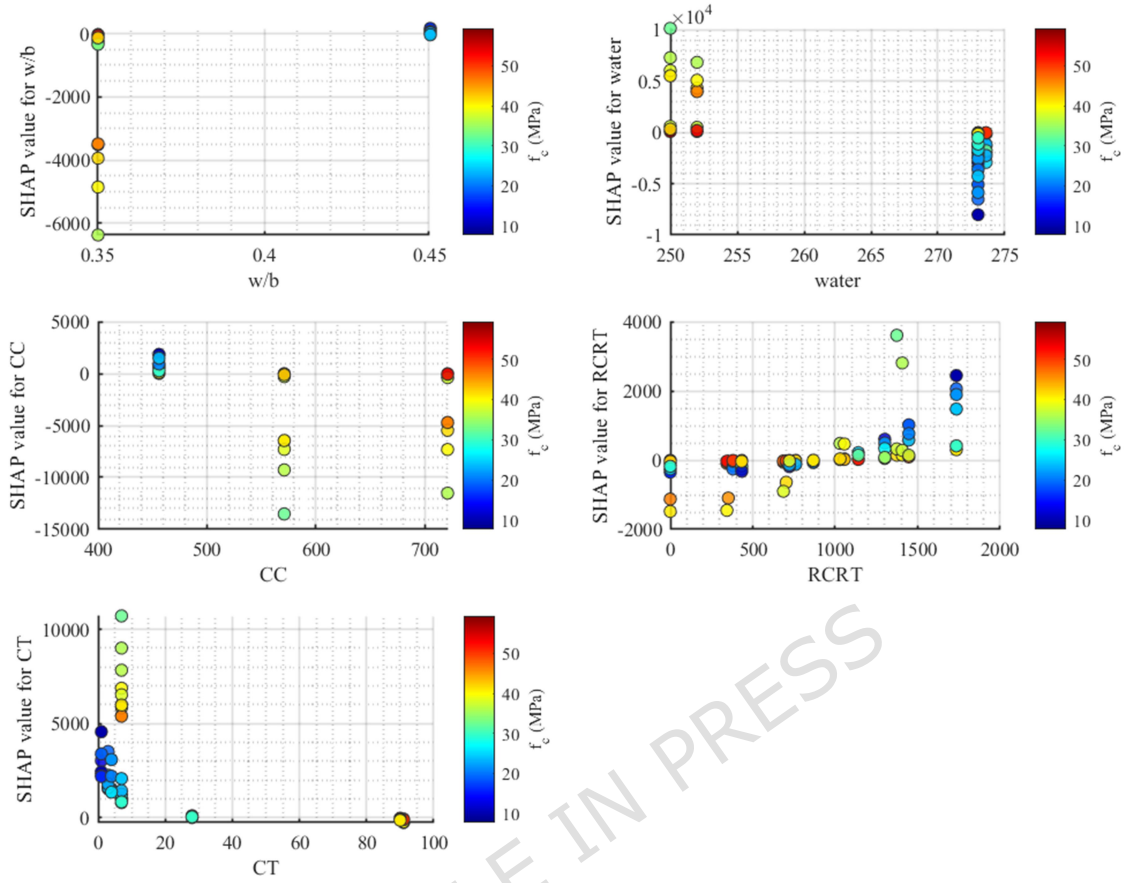

Figure 14. SHAP dependence plots for input variables showing parameter-wise influence patterns on compressive strength.

Overall, the SHAP-based interpretation confirms that water content and curing time dominate the mechanical response of RCRT-modified mortars, while CC, RCRT, and w/b exert more limited but still measurable effects. The combined use of feature contribution scores and dependence plots provides a comprehensive and interpretable assessment of variable importance, ensuring that the sensitivity evaluation is independent of the physical units and scales of the input parameters.

5. Conclusion

In this study, two advanced soft-computing methods, GMDH and GEP, were used to develop accurate and interpretable models for predicting the compressive strength of RCRT-modified mortar. The modeling was based on a dataset of 139 laboratory specimens with key mix-design parameters, including w/b, water content, CC, fly ash, sand, RCRT, and CT. The performance of these two models was **evaluated against** three classical regression methods (LR, NLR, and MLR), and a sensitivity analysis was performed on the selected model.

The results showed that the GMDH model performed much more accurately than the other models, with $R^2 = 0.942$ in the testing phase and low RMSE and MAE values (2.97 and **2.59**, respectively). The network-based structure and automatic node-selection algorithm in GMDH enabled the final model to avoid excessive complexity and achieve high accuracy. In contrast, the GEP model, while providing explicit equations and analytic tree-based structures, also showed acceptable performance but **was still ranked lower** than GMDH in terms of prediction accuracy. Classical regression models, especially the LR model, failed to establish a strong correlation with actual data and performed poorly when faced with nonlinear relationships between input parameters and compressive strength. This highlights the importance of using data-driven and flexible models in analyzing the complex behavior of engineering materials. Due to their white-box nature, GMDH and GEP methods, in addition to accurate prediction, also allow for analyzing relationships between variables and identifying key factors affecting RCRT-modified mortar behavior. This capability **is generally not available** in many black-box methods.

The sensitivity analysis results showed that water content had the most significant impact on the compressive strength of RCRT-modified mortar, **such that even slight variations in this parameter led to notable changes** in the model output. Other parameters, such as CC and CT,

also played an important role, while parameters such as sand and RCRT **had a comparatively smaller influence** on the model output.

This study demonstrated that integrating recycled materials such as RCRT with soft-computing techniques like GMDH and GEP **provides** an effective approach for developing sustainable and high-performance cementitious mortars. These models were able to capture and predict the complex and nonlinear relationships governing compressive strength with high accuracy, with the GMDH model outperforming GEP due to its simpler structure and better interpretability. Sensitivity analysis also showed that variables such as water, CC, and CT **significantly influence** strength. In contrast, the results showed that RCRT has a negative influence on compressive strength; however, within the low-to-moderate replacement levels represented in this dataset, the magnitude of this effect is relatively small and remains secondary compared with the dominant parameters such as water content, curing time, and cement dosage. Based on these observations, RCRT can be incorporated in controlled amounts as an environmentally beneficial fine-aggregate component without causing a considerable reduction in strength. This highlights the potential of RCRT as a sustainable material option in mortar mix design.

In addition, future research may incorporate more advanced machine learning techniques such as Random Forest, XGBoost, or neural network models to further expand the comparative analysis and potentially improve predictive performance.

Funding

The authors received no funding for this work

Data Availability

The datasets generated and/or analyzed during the current study are available from the corresponding author on reasonable request.

Author Contribution declaration

Vahid Ghorbani, Ali Seyedkazemi (corresponding author) and Saman Soleimani Kutanaei contributed to the preparation of all parts of the article

References

[1] Miraldo, S., Lopes, S., Lopes, A. V., & Pacheco-Torgal, F. (2022). Design of fly ash-based alkali-activated mortars, containing waste glass and recycled CDW aggregates, for compressive strength optimization. Materials, 15(3), 1204.

[2] Liu, T., Wei, H., Zou, D., Zhou, A., & Jian, H. (2020). Utilization of waste cathode ray tube funnel glass for ultra-high performance concrete. Journal of Cleaner Production, 249, 119333.

[3] Anwar, M. K., Zhu, X., Gilabert, F. A., & Siddiq, M. U. (2024). Recycling and optimum utilization of CRT glass as building materials: An application of low CO_2 based circular economy for sustainable construction. Construction and Building Materials, 453, 138798.

[4] Cao, Q., Yuan, X., Amin, M. N., Ahmad, W., Althoey, F., & Alsharari, F. (2023). A soft-computing-based modeling approach for predicting acid resistance of waste-derived cementitious composites. Construction and Building Materials, 407, 133540.

[5] Choi, S. Y., Choi, Y. S., & Yang, E. I. (2017). Effects of heavy weight waste glass recycled as fine aggregate on the mechanical properties of mortar specimens. Annals of Nuclear Energy, 99, 372–382.

[6] Ling, T. C., & Poon, C. S. (2013). Effects of particle size of treated CRT funnel glass on properties of cement mortar. Materials and Structures, 46, 25–34.

[7] Ling, T. C., & Poon, C. S. (2011). Utilization of recycled glass derived from cathode ray tube glass as fine aggregate in cement mortar. Journal of Hazardous Materials, 192(2), 451–456.

[8] Ling, T. C., Poon, C. S., Lam, W. S., Chan, T. P., & Fung, K. K. L. (2012). Utilization of recycled cathode ray tubes glass in cement mortar for X-ray radiation-shielding applications. Journal of Hazardous Materials, 199, 321–327.

[9] Bentegri, H., Rabehi, M., Kherfane, S., Nahool, T. A., Rabehi, A., Guermoui, M., ... & El-Kenawy, E. S. M. (2025). Assessment of compressive strength of eco-concrete reinforced using machine learning tools. Scientific Reports, 15(1), 5017.

[10] Ghazavi, M., & Afrakoti, M. T. P. (2025). Unconfined Compressive Strength Prediction of Soils Improved with Biopolymers: Machine Learning Approach. Transportation Infrastructure Geotechnology, 12(1), 1–32.

[11] Dong, Y., Tang, J., Xu, X., Li, W., Feng, X., Lu, C., ... & Liu, J. (2025). A new method to evaluate features importance in machine-learning based prediction of concrete compressive strength. Journal of Building Engineering, 111874.

[12] Liu, Y., Yu, H., Guan, T., Chen, P., Ren, B., & Guo, Z. (2025). Intelligent prediction of compressive strength of concrete based on CNN-BiLSTM-MA. Case Studies in Construction Materials, 22, e04486.

[13] Lu, C., Zhou, C., Yuan, S., Zhang, H., Qian, H., & Fang, Y. (2025). Data-driven compressive strength prediction of basalt fiber reinforced rubberized concrete using neural network-based models. Materials Today Communications, 111706.

[14] Anyaoha, U., Zaji, A., & Liu, Z. (2020). Soft computing in estimating the compressive strength for high-performance concrete via concrete composition appraisal. Construction and Building Materials, 257, 119472.

[15] Asteris, P. G., Skentou, A. D., Bardhan, A., Samui, P., & Lourenço, P. B. (2021). Soft computing techniques for the prediction of concrete compressive strength using Non-Destructive tests. Construction and Building Materials, 303, 124450.

[16] Yang, Y., Tao, Y., Jiang, T., & Zhao, W. (2024). Prediction of bent corner strength of FRP reinforcement based on genetic algorithm. Construction and Building Materials, 449, 138357.

[17] Alotaibi, K. S., & Almohammed, F. (2025). Forecasting interfacial bond strength in FRP-reinforced concrete using soft computing techniques. Construction and Building Materials, 473, 140827.

[18] Ahmad, S. A., Ahmed, H. U., Rafiq, S. K., Gul-Mohammed, J. F., Ahmed, D. A., Rostam, K. J., & Fqi, K. O. (2024). Exploring the influence of waste glass granular replacement on compressive strength in concrete mixtures: A normalization and modeling study. Journal of Building Pathology and Rehabilitation, 9(1), 52.

[19] Feridoni, P., Seyedkazemi, A., Kutanaei, S. S., & Davoudi-Kia, A. (2025). Modeling and sensitivity analysis of the compressive strength of recycled brick aggregates concrete using GMDH, GEP and RSM methods. Results in Engineering, 104891.

[20] Hoseini, S., Seyedkazemi, A., Davoudi-Kia, A., & Kutanaei, S. S. (2025). A data mining approach for proposing a relationship to predict self-compaction concrete crack width after the self-healing period. Results in Engineering, 104980.

[21] Liong, S. Y., Lim, W. H., & Paudyal, G. N. (2000). River stage forecasting in Bangladesh: Neural network approach. Journal of Computing in Civil Engineering, 14(1), 1–8.

de-Prado-Gil, J., Palencia, C., Jagadesh, P., & Martínez-García, R. (2022). A study on the prediction of compressive strength of self-compacting recycled aggregate concrete utilizing novel computational approaches. Materials, 15(15), 5232.

de-Prado-Gil, J., Martínez-García, R., Jagadesh, P., Juan-Valdés, A., Gonzalez-Alonso, M. I., & Palencia, C. (2024). To determine the compressive strength of self-compacting recycled aggregate concrete using artificial neural network (ANN). Ain Shams Engineering Journal, 15(2), 102548.

Jagadesh, P., de Prado-Gil, J., Silva-Monteiro, N., & Martinez-Garcia, R. (2023). Assessing the compressive strength of self-compacting concrete with recycled aggregates from mix ratio using machine learning approach. Journal of Materials Research and Technology, 24, 1483-1498.

de-Prado-Gil, J., Palencia, C., Jagadesh, P., & Martínez-García, R. (2022). A comparison of machine learning tools that model the splitting tensile strength of self-compacting recycled aggregate concrete. Materials, 15(12), 4164.

Ghazavi, M., Rouhani, M., & Khoshghalb, A. (2025). Analytical Method for Estimating the Bearing Capacity of Stone Column Groups. International Journal of Geomechanics, 25(8), 04025164.

Ghazavi, M., Rouhani, M., & Khoshghalb, A. (2024). Evaluation of the methods used for estimating the bearing capacity of stone columns. Transportation Geotechnics, 49, 101405.

Ling, T. C., & Poon, C. S. (2012). A comparative study on the feasible use of recycled beverage and CRT funnel glass as fine aggregate in cement mortar. Journal of cleaner production, 29, 46-52.

Zhao, H., & Poon, C. S. (2017). A comparative study on the properties of the mortar with the cathode ray tube funnel glass sand at different treatment methods. Construction and Building Materials, 148, 900-909.

Wan, Z., Xu, Y., & Šavija, B. (2021). On the use of machine learning models for prediction of compressive strength of concrete: influence of dimensionality reduction on the model performance. Materials, 14(4), 713.

Ashraf, M. W., Khan, A., Tu, Y., Wang, C., Ben Kahla, N., Javed, M. F., ... & Tariq, J. (2024). Predicting mechanical properties of sustainable green concrete using novel machine learning: Stacking and gene expression programming. Reviews on Advanced Materials Science, 63(1), 20240050.

Shuai, J., Zhang, J., Cui, Z., Yu, D., Libing, J., & Bingquan, S. (2025). Compressive Strength Prediction of Machine-Made Sand Concrete Based on a Bayesian Optimization-Stacking Model. Case Studies in Construction Materials, e05516.

Shanthi Vengadeshwari, R., Ujwal, M. S., Shiva Kumar, G., Mahesh, R., Sanjay, N., Rajiv, K. N., & Pandit, P. (2025). SHAP-based prediction and optimization of compressive strength in M30 concrete with dry sewage sludge as fine aggregate replacement. Discover Materials, 5(1), 183.

Meng, S., Shi, Z., Xia, C., Zhou, C., & Zhao, Y. (2025, January). Exploring LightGBM-SHAP: Interpretable predictive modeling for concrete strength under high temperature conditions. In Structures (Vol. 71, p. 108134). Elsevier.

Ivakhnenko, A. G. (2007). Polynomial theory of complex systems. IEEE transactions on Systems, Man, and Cybernetics, (4), 364-378.

Ivakhnenko, A. G., & Ivakhnenko, G. A. (1995). The review of problems solvable by algorithms of the group method of data handling (GMDH). Pattern recognition and image analysis c/c of raspoznavaniye obrazov i analiz izobrazhenii, 5, 527-535.

Farlow, S. J. (2020). The GMDH algorithm. In Self-organizing methods in modeling (pp. 1-24). CrC Press.

Babin, A. S., Baryshnikov, M. I., & Gapanyuk, Y. E. (2025, April). Group Method of Data Handling (GMDH) in Forecasting Electric Power Consumption. In 2025 7th International Youth Conference on Radio Electronics, Electrical and Power Engineering (REEPE) (pp. 1-6). IEEE.

Ferreira, C. (2001). Gene expression programming: a new adaptive algorithm for solving problems. arXiv preprint cs/0102027.

Ferreira, C. (2006). Gene expression programming: mathematical modeling by an artificial intelligence (Vol. 21). Springer.

Faraz, M. I., Arifeen, S. U., Amin, M. N., Nafees, A., Althoey, F., & Niaz, A. (2023, July). A comprehensive GEP and MEP analysis of a cement-based concrete containing metakaolin. In Structures (Vol. 53, pp. 937-948). Elsevier.

Ghanizadeh, A. R., Safi Jahanshahi, F., & Naser Alavi, S. (2024). Application of gene expression programming for modeling bearing capacity of aggregate pier reinforced clay. International Journal of Mining and Geo-Engineering, 58(1), 113-119.

Alabduljabbar, H., Khan, M., Awan, H. H., Eldin, S. M., Alyousef, R., & Mohamed, A. M. (2023). Predicting ultra-high-performance concrete compressive strength using gene expression programming method. Case Studies in Construction Materials, 18, e02074.

Ferreira, C. (2009). Gene expression programming and the evolution of computer programs. In Medical Informatics: Concepts, Methodologies, Tools, and Applications (pp. 2154-2173). IGI Global Scientific Publishing.

Ahmad, A., Chaiyasarn, K., Farooq, F., Ahmad, W., Suparp, S., & Aslam, F. (2021). Compressive strength prediction via gene expression programming (GEP) and artificial neural network (ANN) for concrete containing RCA. Buildings, 11(8), 324.

Kontoni, D. P. N., Onyelowe, K. C., Ebid, A. M., Jahangir, H., Rezazadeh Eidgahee, D., Soleymani, A., & Ikpa, C. (2022). Gene expression programming (GEP) modelling of sustainable building materials including mineral admixtures for novel solutions. Mining, 2(4), 629-653.

Aslam, F., Farooq, F., Amin, M. N., Khan, K., Waheed, A., Akbar, A., ... & Alabdulijabbar, H. (2020). Applications of gene expression programming for estimating compressive strength of high-strength concrete. Advances in Civil Engineering, 2020(1), 8850535.

Elshaarawy, M. K., Alsaadawi, M. M., & Hamed, A. K. (2024). Machine learning and interactive GUI for concrete compressive strength prediction. Scientific Reports, 14(1), 16694.

Gao, X., Yao, X., Xie, R., Li, X., Cheng, J., & Yang, T. (2022). Performance of fly ash-based geopolymer mortars with waste cathode ray tubes glass fine aggregate: A comparative study with cement mortars. Construction and Building Materials, 344, 128243.

Mahmoud, A. A., El-Sayed, A. A., Aboraya, A. M., N. Fathy, I., & Nabil, I. M. (2025). Enhancing predictive accuracy of nano-additive concrete gamma ray attenuation at high temperatures using AI-based models. Neural Computing and Applications, 1-34.

Dahish, H. A., Alkharisi, M. K., Abouelnour, M. A., Fathy, I. N., Sadawy, M. A., & Mahmoud, A. A. (2025). Predicting the Compressive Strength of Waste Powder Concrete Using Response Surface Methodology and Neural Network Algorithm. Buildings, 15(21), 3934.

Fathy, I. N., Dahish, H. A., Alkharisi, M. K., Mahmoud, A. A., & Fouad, H. E. E. (2025). Predicting the compressive strength of concrete incorporating waste powders exposed to elevated temperatures utilizing machine learning. Scientific Reports, 15(1), 25275.

Mahmoud, A. A., El-Sayed, A. A., Aboraya, A. M., Fathy, I. N., Zygouris, N., Sadollah, A., ... & Asteris, P. G. (2025). Synergizing machine learning and experimental analysis to predict post-heating compressive strength in waste concrete. Structural Concrete.

Zeyad, A. M., Mahmoud, A. A., El-Sayed, A. A., Aboraya, A. M., Fathy, I. N., Zygouris, N., ... & Agwa, I. S. (2024). Compressive strength of nano concrete materials under elevated temperatures using machine learning. Scientific Reports, 14(1), 24246.

Zhang, Y., Ren, W., Chen, Y., Mi, Y., Lei, J., & Sun, L. (2024). Predicting the compressive strength of high-performance concrete using an interpretable machine learning model. Scientific Reports, 14(1), 28346.

Aksu, G., Güzeller, C. O., & Eser, M. T. (2019). The effect of the normalization method used in different sample sizes on the success of artificial neural network model. International journal of assessment tools in education, 6(2), 170-192.

Safieh, H., Hawileh, R. A., Assad, M., Hajjar, R., Shaw, S. K., & Abdalla, J. (2024). Using multiple machine learning models to predict the strength of uhpc mixes with various fa percentages. Infrastructures, 9(6), 92.

Raju, M. R., Rahman, M., Islam, M. M., Hasan, N. M. S., Hasan, M. M., Sharmily, T., & Hosen, M. S. (2024). A Comparative Analysis of Machine Learning Approaches for Evaluating the Compressive Strength of Pozzolanic Concrete. IUBAT Review, 7(1), 90-122.

Moshaver, E., Seyedkazemi, A., & Jahangir, S. (2025). Innovative approaches for predicting the elastic modulus and tensile strength of green concrete using soft computing methods. Scientific Reports, 15(1), 42743.

Fereidouni, P., Seyedkazemi, A., Kutanaei, S. S., & Davoudi-Kia, A. (2025). Modeling and sensitivity analysis of the compressive strength of recycled brick aggregates concrete using GMDH, GEP and RSM methods. Results in Engineering, 26, 104891.

Hosseini, S., Seyedkazemi, A., Davoudi-Kia, A., & Kutanaei, S. S. (2025). A data mining approach for proposing a relationship to predict self-compaction concrete crack width after the self-healing period. Results in Engineering, 26, 104980.

Amar, M. N., & Ghahfarokhi, A. J. (2020). Prediction of CO2 diffusivity in brine using white-box machine learning. Journal of Petroleum Science and Engineering, 190, 107037.

MolaAbasi, H., Khajeh, A., & Jamshidi Chenari, R. (2021). Use of GMDH-type neural network to model the mechanical behavior of a cement-treated sand. Neural Computing and Applications, 33(22), 15305-15318.

Madandoust, R., Bungey, J. H., & Ghavidel, R. (2012). Prediction of the concrete compressive strength by means of core testing using GMDH-type neural network and ANFIS models. Computational Materials Science, 51(1), 261-272.

Madandoust, R., Ghavidel, R., & Nariman-Zadeh, N. (2010). Evolutionary design of generalized GMDH-type neural network for prediction of concrete compressive strength using UPV. Computational Materials Science, 49(3), 556-567.

MolaAbasi, H., Khajeh, A., & Jamshidi Chenari, R. (2021). Use of GMDH-type neural network to model the mechanical behavior of a cement-treated sand. Neural Computing and Applications, 33(22), 15305-15318.

Pham, V. N. (2025). Practical formulation for estimating the compressive strength of self-compacting fly ash concrete using gene-expression programming. Journal of Science and Technology in Civil Engineering (JSTCE)-HUCE, 19(3), 98-109.

Ashrafian, A., Gandomi, A. H., Rezaie-Balf, M., & Emadi, M. (2020). An evolutionary approach to formulate the compressive strength of roller compacted concrete pavement. Measurement, 152, 107309.

Khan, M. A., Aslam, F., Javed, M. F., Alabduljabbar, H., & Deifalla, A. F. (2022). New prediction models for the compressive strength and dry-thermal conductivity of bio-composites using novel machine learning algorithms. Journal of Cleaner Production, 350, 131364.

Abouelnour, M. A., Fathy, I. N., Mahmoud, A. A., Alturki, M., Abdelaziz, M. M., Mostafa, S. A., ... & Fattouh, M. S. (2025). Valorization of nano additives effects on the physical, mechanical and radiation shielding properties of high strength concrete. Scientific Reports, 15(1), 14440.

Mahmoud, A. A., El-Sayed, A. A., Fathy, I. N., Fawzy, S., Alturki, M., Elfakharany, M. E., ... & Nabil, I. M. (2025). Evaluation of rice husk biochar influence as a partial cement replacement material on the physical, mechanical, microstructural, and radiation shielding properties of ordinary concrete. Scientific Reports, 15(1), 27229.

Fattouh, M. S., Abouelnour, M. A., Mahmoud, A. A., Fathy, I. N., El Sayed, A. F., Elhameed, S. A., & Nabil, I. M. (2025). Impact of modified aggregate gradation on the workability, mechanical, microstructural and radiation shielding properties of recycled aggregate concrete. Scientific Reports, 15(1), 18428.